



# The frequency degeneracy range of transverse mode in an off-axis end-pumped solid-state lasers

Jia'ning Li<sup>1,3</sup> · Shengbo Song<sup>1,3</sup> · Gang Huang<sup>1,4</sup> · Pengfei Zhou<sup>1,3</sup> · Zeqian Jiang<sup>1,4</sup> · Pengjian Xie<sup>1,5</sup> · Wenbin Liao<sup>1,2,4</sup> · Zhanglang Lin<sup>1,2</sup> · Bingxuan Li<sup>1,2,4</sup> · Ge Zhang<sup>1,2,4</sup>

Received: 12 March 2024 / Accepted: 18 April 2024 / Published online: 4 May 2024  
© The Author(s), under exclusive licence to Springer-Verlag GmbH Germany, part of Springer Nature 2024

## Abstract

In this work, the degenerate phenomena of transverse mode's frequency in an off-axis end-pumped solid-state lasers was researched based on a semi-confocal cavity. When the off-axis distance was 0.05 mm, the beam profile was always nearly Hermite-Gaussian mode in the change of cavity length. At this time, the degenerate range of transverse modes was the cavity length to radius ratio  $L/R$  from 0.4974 to 0.5008 by the analysis of the frequency signals. When the off-axis distance was 0.10 mm, the beam profile changed from the Hermite-Gaussian mode to the geometric mode and finally back to the Hermite-Gaussian mode as cavity length varied. At this time, the degenerate range of transverse modes was  $L/R$  from 0.4974 to 0.5025 by the analysis of the frequency signals. The beam profile was nearly the geometric mode in the range of  $L/R$  from 0.4958 to 0.5092. The degeneracy range by observing beating frequency changes was more accurate and more useful than the method by comparing the beam profile changes. Furthermore, it was found that the off-axis pumping did not significantly alter the degeneracy position and range.

## 1 Introduction

Under the principle of paraxial approximation, laser transverse modes in spherical cavities exhibit various eigenmodes, such as Hermite-Gaussian (HG) modes in cartesian coordinate and Laguerre-Gaussian (LG) modes in cylindrical coordinate [1, 2]. Numerous theoretical frameworks

and experimental results suggested that the special forms of structured light were able to be synthesized within the spherical resonator [3–5]. Shu-Chun Chu et al. inserted a fine opaque-wire into the laser resonator for exciting all high-order HG modes [3]. Ajian Hu et al. obtained all kinds of LG modes by controlling the locations and thicknesses of opaque rings and lines on the mask [4]. These structured lights could be applied in many fields, such as trapping nanoparticles [6], optical communication and optical device [7]. Researchers were able to be obtained more complex structured light by using the principle of transverse mode degeneracy in lasers. Innumerable effort has been devoted to researching the degenerate phenomena of transverse modes in recently two decades [8–15]. Many researchers considered that the transverse mode degeneracy was the result of the frequency locking of transverse modes [12–14, 16]. Other researchers thought that the transverse mode degeneracy was the result of the phase locking of transverse modes [17]. As for the frequency degenerating of transverse modes, theory and results of it had been researched substantially [13, 14, 16, 18, 19]. Chen Y.F., Tung J.C and Lu T.H. et al. obtained the Lissajous modes [19, 20] and Multi-axis Hermite-Laguerre-Gaussian mode [21] by the transverse mode degenerate. These experiments focus on the analysis of the

✉ Bingxuan Li  
libingxuan@fjirsm.ac.cn

✉ Ge Zhang  
zhg@fjirsm.ac.cn

<sup>1</sup> Key Laboratory of Optoelectronic Materials Chemistry and Physics, Fujian Institute of Research on the Structure of Matter, Chinese Academy of Sciences, Fuzhou 350002, Fujian, China

<sup>2</sup> Fujian Science & Technology Innovation Laboratory for Optoelectronic Information of China, Fuzhou 350108, Fujian, China

<sup>3</sup> College of Chemistry and Materials, Fujian Normal University, Fuzhou 350117, Fujian, China

<sup>4</sup> University of Chinese Academy of Science, Beijing 100049, China

<sup>5</sup> College of Chemistry, Fuzhou University, Fuzhou 350108, Fujian, China

phenomenon after degeneracy in the resonator. However, there were few researches on how wide the stable degenerate region was, to our knowledge. If there were some methods to analyze the detailed degeneracy process in the resonator, it will greatly promote the practical applications of the transverse modal degeneracy. It could help to judge whether the degenerate phenomena occurred or not. And the stable degenerate region was a necessary condition when exploiting the mechanism of frequency degenerating to realize transverse mode locking. Therefore, research on the detailed degenerate process of modes and the stable degenerate region held great significance.

The theory of fractional degenerate configuration of resonant cavity was able to explain the experimental phenomenon during the frequency degenerating process of transverse modes [19]. There were studies focusing on fractional degenerate resonator configurations [13, 14, 22–24]. Chen Y.F. et al. considered that the transverse modes in the spherical cavity were identical to the eigenfunctions in the 2D isotropic harmonic oscillator [25]. They also used the 2D Gaussian wave-packet state to analyze the phenomena of transverse modes degenerate [2]. These studies suggested that laser modes localized on geometrical trajectories were formed by a frequency locking of nondegenerate transverse modes with different longitudinal orders [22]. These studies explicitly showed the results of frequency degenerating of transverse modes, and provided rational explanations to the results referring to the theory of frequency degenerating. J. Dingjan, M.P. van Exter, J.P. Woerdman et al. measured the total power output of the laser at constant pump power against the scaled resonator length  $L/R$  [26]. But these studies did not describe the detailed degenerate process and the stable degenerate region, which were important in actual application.

In this work, we analyzed theoretically and experimentally the phenomena of transverse mode's degenerate near the semi-confocal cavity with different off-axis distances. The position and range of transverse mode degeneracy in the resonator were analyzed by using the change process of frequency signal and the change of beam profile patterns. By analyzing these phenomena, it was found that the off-axis distance did not change obviously the position and range of the degeneracy cavity configuration. The exact position and range of degenerate cavity length were able to be found by analyzing the change of frequency signal in the process of cavity length change. However, the exact position and range of degenerate cavity length couldn't be analyzed by the change of beam profile patterns. Therefore, it was feasible and effective to analyze the position and range of transverse mode degeneracy by observing the changes of the transverse mode frequency signal.

## 2 Theoretical model

The path of light ray in a stable spherical resonator can be described by the ABCD transmission matrix [27]. The round-trip propagation matrix starting from a flat-concave cavity with a flat input mirror at  $z = 0$  and a concave output coupler with  $R$  radius of curvature at  $z = L$  is [2, 27]:

$$M = \begin{pmatrix} 1 & 0 \\ 0 & 1 \end{pmatrix} \begin{pmatrix} 1 & L \\ 0 & 1 \end{pmatrix} \begin{pmatrix} 1 & 0 \\ -\frac{2}{R} & 1 \end{pmatrix} \begin{pmatrix} 1 & L \\ 0 & 1 \end{pmatrix} = \begin{pmatrix} 1 - \frac{2L}{R} & 2L - \frac{2L^2}{R} \\ -\frac{2}{R} & 1 - \frac{2L}{R} \end{pmatrix} \quad (1)$$

Let the coordinate vector of the light be  $\vec{x} = [x \ \theta]^T$ , where 'x' represents the initial coordinate of the light and 'θ' is the transmission direction of the light. The condition for achieving a stable transverse mode in the resonator is that there exist any transverse patterns will return one round-trip later with exactly the same pattern. With  $|M| = 1$ , Two eigenvalues of the matrix  $M$  can be found to be [2, 27, 28]:

$$\lambda_{\pm} = \frac{A+D}{2} \pm \sqrt{\left(\frac{A+D}{2}\right)^2 - (AD-BC)} = \exp(\pm i\varphi) \quad (2)$$

The medium of ray transformations is air so the condition for  $AD - BC = 1$  is satisfied. When  $A + D \leq 2$ , the eigenvalues are Imaginary number.  $\varphi$  is the Gouy phase angle in a round-trip of the light ray transformations. The Gouy phase angle is related to the resonator configuration according to [2, 27]:

$$\cos(\varphi) = \frac{A+D}{2} = 1 - \frac{2L}{R} \quad (3)$$

When the resonator is in a hemi-confocal geometry for which the Gouy phase angle  $\varphi = 2\pi(1/4)$ , the output laser modes are the geometric modes. A prominent feature of the transverse beam profile is the presence of fringes in both the near and far fields. In the paraxial approximation, where we can find the propagation of rays inside the cavity using the ABCD-matrix formalism, we find that any ray inside the cavity will reproduce, and hence form a closed trajectory, after  $Q$  round-trips [26]. This is the direct result from the fact that the ABCD matrix for such a resonator satisfies.

$$\begin{pmatrix} A & B \\ C & D \end{pmatrix}^Q = \begin{pmatrix} 1 & 0 \\ 0 & 1 \end{pmatrix} \quad (4)$$

The cavity length corresponding to a semi-confocal cavity is the condition for  $L = R/2$ , which means that the 1/4 degenerate resonant cavity configuration in  $\Delta f_T / \Delta f_L = \varphi / 2\pi = 1/4$ . The frequencies of Hermite-Gaussian modes native to a spherical mirror resonator are given by [26]:

$$f_{q,n,m} = \frac{c}{2L} \left[ q + (n + m + 1) \frac{\varphi}{2\pi} \right] \tag{5}$$

In the above formula,  $q$  is the longitudinal mode index,  $n$  and  $m$  are the transverse mode indices,  $c$  is the speed of light. If the frequencies of the two modes degenerate, the frequency of the modes satisfies that:

$$f_{q,n,m} = f_{q-\Delta q, n+\Delta n, m+\Delta m} \tag{6}$$

When the sum of  $n$  and  $m$  is constant, the frequency difference between two orders longitudinal modes is:

$$\Delta f_L = \frac{c}{2L} \tag{7}$$

When  $q$  is constant, the frequency difference between two orders transverse modes is:

$$\Delta f_T = \frac{c}{2L} * \frac{\varphi}{2\pi} \tag{8}$$

$\Delta f_L$  indicates the transverse mode spacing and  $\Delta f_T$  indicates longitudinal mode spacing. The ratio of transverse mode spacing to longitudinal mode spacing is:

$$\frac{\Delta f_T}{\Delta f_L} = \frac{\varphi}{2\pi} = \frac{1}{2\pi} * \cos^{-1} \left( 1 - \frac{2L}{R} \right) \tag{9}$$

From Eq. (9) we see that the ratio of transverse mode spacing to longitudinal mode spacing depends on the ratio  $L/R$ . The feature of  $\Delta f_T/\Delta f_L = P/Q$  means that the laser resonator is in the degenerate condition of  $P/Q$ , which  $P$  and  $Q$  are coprime positive integers. Taking the  $1/4$  degenerate resonant cavity configuration as an example, a frequency signal packet with  $\Delta f_T$  and another frequency signal packet with  $\Delta f_L - 3\Delta f_T$  can coincide. The schematic model of modes frequency degeneracy in the resonator is shown in the Fig. 1:

### 3 Experimental setup

In this work, the method of the off-axis pumping was used to generate pure high-order modes in a plano-concave cavity. The experimental setup was illustrated in Fig. 2. The 808 nm pump beam emitted by a fiber-coupled diode laser with a 200  $\mu\text{m}$  diameter of fiber core was collimated by 2 lens L1 ( $f=50$  mm) and L2 ( $f=46$  mm). They were fixed together on a three-dimensional displacement platform. The laser resonator was composed of one flat mirror IM employed as the pump mirror and one concave mirror ( $R_{OC}=50$  mm,  $T=10\%$ ) employed as the output coupler (OC). The OC was fixed to a one-dimensional displacement platform in order to control the resonator cavity length. The gain medium was an a-cut  $3 \times 3 \times 3$  mm<sup>3</sup> 0.8% at. Nd:YVO<sub>4</sub> crystal. The output beam passed through a filter (F) to get rid of the pump beam and was split into two beams by a beam splitter (BS) where one of them was used to record the beam profile by an IR camera (DataRay, Inc.) and another was used to record the beating frequency by a radio frequency (RF) spectrum analyzer (Keysight, Inc. N9000A, a bandwidth of 9 kHz to 13.6 GHz). The length of the cavity was varied between 23 and 27 mm, to select either frequency-degenerate or non-frequency-degenerate configurations. The significant point

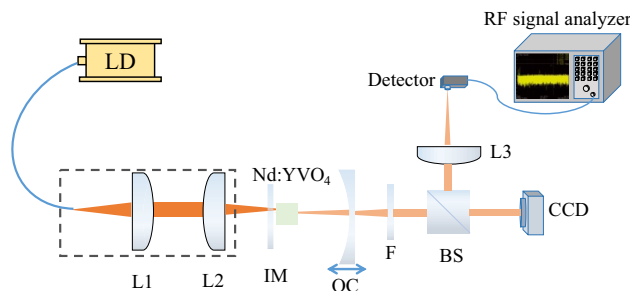
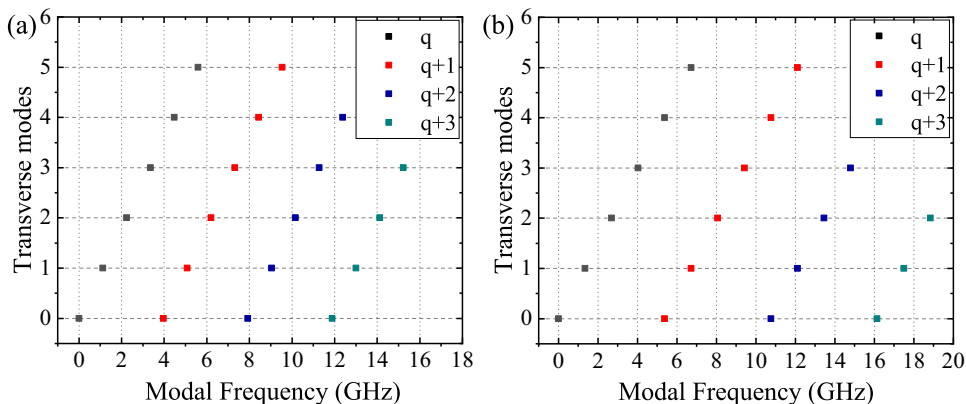


**Fig. 2** A sketch of experimental set up for this Nd:YVO<sub>4</sub> laser: LD, laser diode; L1-L3, lenses; IM, input pump mirror; OC, output coupler; F, filter; BS, beam splitter

**Fig. 1** The schematic model of modes frequency degeneracy in the resonator. Different colors represent different longitudinal modes and different points in the same color represent different orders of transverse modes in the same longitudinal modes. The horizontal coordinate represents the mode frequency. **a**  $L/R=0.7$ , **b**  $L/R=0.5$



was that the pump spot on the crystal is displaced from the axis of the system by a distance.

## 4 Results and discussion

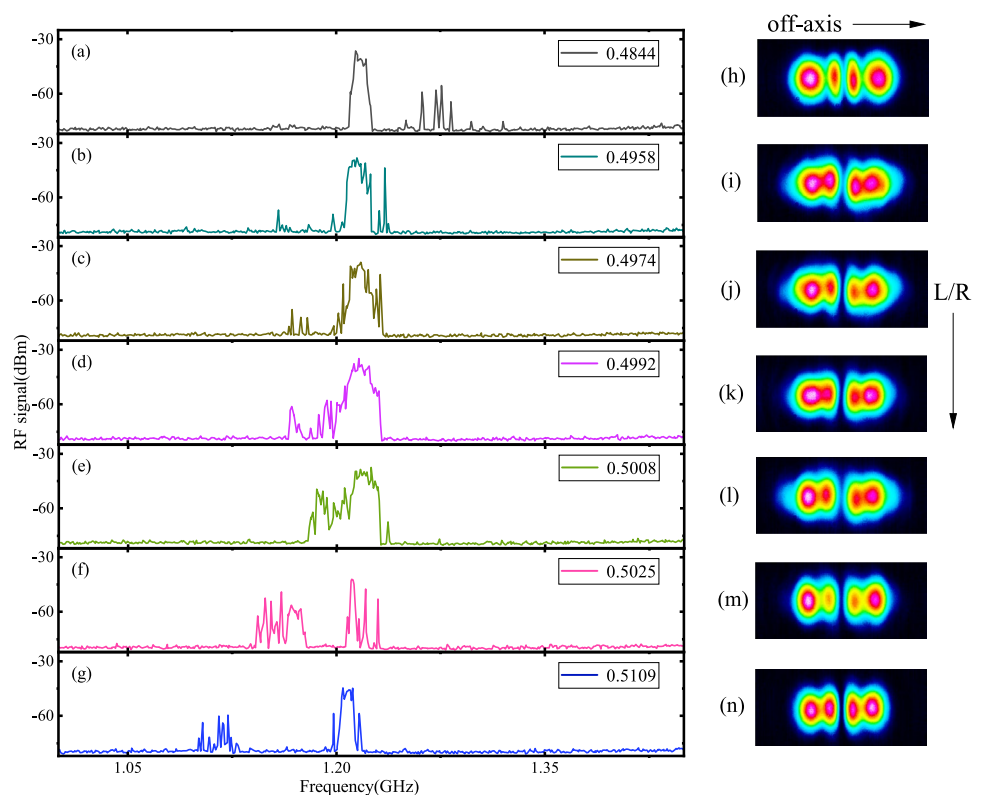
In the case of not selecting a frequency-degenerate cavity, off-axis pumping method will induce directly the higher-order HG model [29, 30]. This method is simple and easy to operate, because it can induce strong gain guiding effects, which are easily manipulated [26]. The strength of the gain guide does not primarily depend on the size of the fundamental Gaussian mode waist. However, the strength of the gain guide rather depends on the position of the pump spot relative to the position of the outermost lobes of high-order HG mode. Compared to on-axis pumping, off-axis pumping method need a broader range of guiding strengths. The resonator mode matched the beam waist radius of 100 microns and the typical threshold power is 0.4 W–0.6 W.

In this experiment, we observed the process of two sets of frequency packets approaching, merging and then moving away. The degeneracy range of transverse modes in the resonator was determined by analyzing the cavity length range when the frequency packets were combined. Considering that the degenerate state of the resonator can be analyzed using the Gouy phase angle that depends on the ratio of cavity length to radius  $L/R$ , we use the ratio of the calculated

cavity length to the curvature radius of the spherical mirror as the control parameter for analysis.

When the off-axis distance in the  $y$  direction was 0.05 mm and the cavity length to radius ratio  $L/R$  was 0.4844, the laser transverse mode's pattern was nearly  $HG_{03}$ . The beating frequency signal intensity changes with  $L/R$  were shown in Fig. 3a–g. Figure 3h–n showed that the change process of laser transverse mode's patterns with  $L/R$  movement. We chose to observe at the threshold pump power of 0.42 W. When  $L/R$  was 0.4958, the two frequency packets were nearly coincident. At this time, weak light appeared on both sides of the spot, and adhesion would occur between the outer and inner lobes, resulting in less obvious dark lines. When  $L/R$  was 0.4974, the two frequency packets were exactly coincident. However, the beam profile pattern had not changed much and remained close to  $HG_{03}$ . According to the research of Chen Y.F. et al., when the order of transverse modes was not high enough, the mode distribution at the position of P/Q degenerate resonator could not show the characteristics of ray trajectory [2]. However, the close combination and separation of the two frequency packets could still be seen from the analysis of the laser RF signal. Furthermore, the location and range of degenerate region could be found by this method. When  $L/R$  was 0.5025, the two frequency packets were separated and the resonator exited the 1/4 degenerated condition. By analyzing the shape change of the beam profile patterns, it could be found that

**Fig. 3** When the off-axis distance was 0.05 mm with different  $L/R$ , a–g were the schematic diagram of frequency signal changes within 1 GHz to 1.45 GHz in the maximum holding state of the radio frequency signal analyzer and h–n were the beam profile patterns captured by CCD

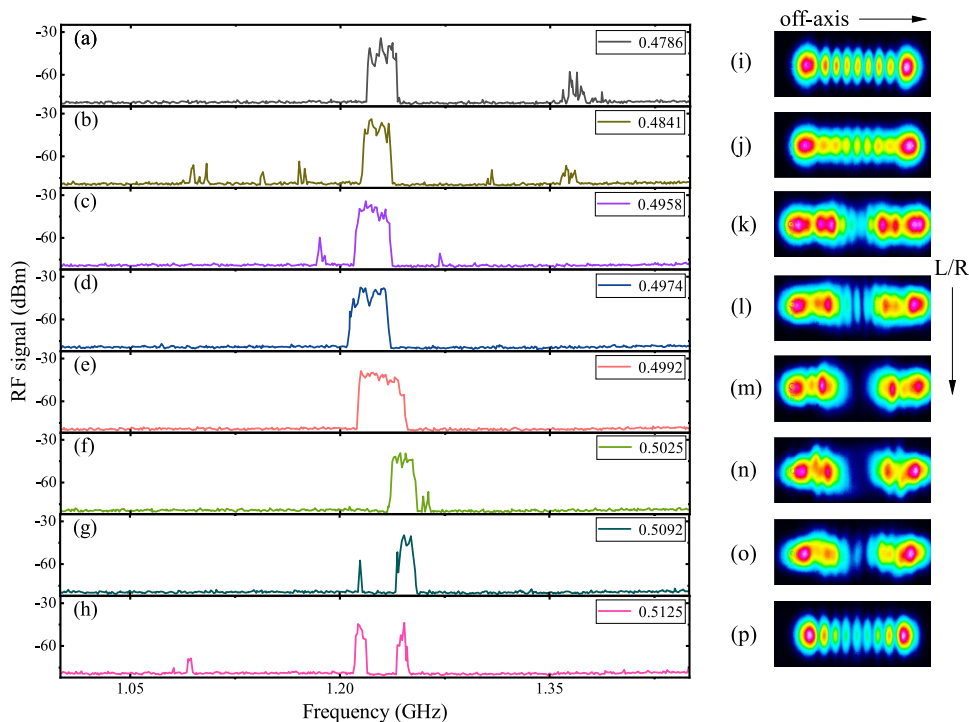


the beam profile was close to  $HG_{03}$  regardless of the length of the resonator. This was because the characteristics of ray trajectory were not displayed under this off-axis amount. In other words, the 1/4 degenerate resonant cavity configuration had few effects for the output laser mode. The results show that the 1/4 degeneracy configuration has little effect on the shape of the output beam profile. The merger range of the 1/4 degenerate resonant cavity configuration in this experiment was about 0.4974 to 0.5008 for the cavity length to radius  $L/R$ .

When the off-axis distance increased to 0.10 mm and the ratio  $L/R$  returned to 0.4786, the beam profile pattern was nearly  $HG_{08}$ . Figure 4a–h showed the beating frequency signal intensity changes with the ratio  $L/R$ . Figure 4i–p showed the changing processes of the beam profile patterns. We chose to observe at the threshold pump power of 0.6 W. When  $L/R$  was 0.4958, the beam profile patterns had begun changed from  $HG_{08}$  to the geometric mode. The intensity of the beam profile center decreased and the intensity of both sides increased. At this time, many packets of RF frequency signal appeared on the analyzer. When  $L/R$  was 0.4974, a main signal appeared on the RF frequency signal analyzer. By observing the changes on the analyzer, it could be considered that the cavity length entered the 1/4 degenerate condition at this time. When  $L/R$  was 0.4992, the intensity at the center of the beam profile disappeared. At this time, the beam

profile pattern completely changed to the geometric mode. When  $L/R$  was 0.5092, a frequency signal suddenly appeared on the left side of the main frequency packet and began away to degeneracy. At this time, the beam profile patterns had begun to change into the  $HG_{08}$ . The intensity at the center of the beam profile pattern increased and the intensity at both sides decreased gradually. By observing the signal changes of the analyzer, it was believed that the length of the resonant cavity had exited the 1/4 degeneracy condition. When  $L/R$  was 0.5125, the two frequency packets gradually moved away from each other. At this time, the beam profile pattern changed back to the  $HG_{08}$ . By observing signal changes on the analyzer, the length range of the resonant cavity where transverse mode's degenerate occurs at this off-axis distance was  $L/R$  from 0.4974 to 0.5025. However, the beam profile patterns began to change long before the frequency signals merged. We speculate that at this off-axis distance, there were some orders of nondegenerate transverse modes with different longitudinal orders degenerated due to frequency locking before the length of resonator reached the 1/4 degeneracy condition. Therefore, it was impossible to determine the accurate length of resonator cavity at the 1/4 degeneracy condition. Furthermore, the changes in the beam profile patterns could not represent that the length of resonator was in a degeneracy condition. Compared to the result with an off-axis distance of 0.05 mm, the cavity length of the 1/4 degeneracy condition had no change.

**Fig. 4** When the off-axis distance was 0.10 mm with different  $L/R$ , a–h were the schematic diagram of frequency signal changes within 1 GHz in the maximum holding state of the radio frequency signal analyzer and i–p were the beam profile patterns captured by CCD





## 5 Conclusion

In summary, it is feasible to observe and analyze the frequency degeneracy of the transverse mode in resonator from the changes of frequency signal. In these experiments, we analyzed the transverse mode's degenerate phenomena by observing the phenomena that the RF signals in the analyzer transformed within the change of cavity length, and that beam profile patterns changed from HG mode to geometric mode and finally back to HG mode. Different orders of nondegenerate transverse modes with different longitudinal orders degenerated when the cavity length was in the 1/4 degeneracy condition. At two different off-axis distances, the range of the resonator cavity length in the 1/4 degeneracy condition was slightly different. At the off-axis distance of 0.05 mm, two packets of frequency signal in the analyzer were coincidence when the range of  $L/R$  was 0.4974–0.5008. At this time, the beam profile patterns were nearly  $HG_{03}$  regardless of the length of the resonator. At the off-axis distance of 0.10 mm, two packets of frequency signal in the analyzer were coincidence when the range of  $L/R$  was 0.4974–0.5025. At this time, the beam profile patterns had obviously changed before the merging of two packets of frequency signal. In short, the degeneracy range by observing beating frequency changes is more accurate and more useful than the method by comparing the transverse pattern changes. This work had some reference value for studying the transverse mode's degeneracy of the resonator cavity.

**Author contributions** Jia'ning Li: Investigation (lead); Data curation (lead); Formal analysis (lead); Methodology (equal); Writing—original draft (lead); Writing—review and editing (equal). Shengbo Song: Writing—review and editing (equal). Gang Huang: Writing—review and editing (equal); Methodology (equal). Pengfei Zhou: Writing—review and editing (equal). Zeqian Jiang: Writing—review and editing (equal). Pengjian Xie: Writing—review and editing (equal). Wenbin Liao: Resources (equal). Zhanglang Lin: Resources (equal). Bingxuan Li: Resources (equal); Writing—review and editing (equal). Ge Zhang: Methodology (equal); Conceptualization (equal); Supervision (lead); Funding acquisition (lead); Project administration (equal); Writing—review and editing (equal).

**Funding** This work was supported the Youth Innovation Promotion Association CAS (2022303), CAS Key Technology Talent Program (2022000061), National Natural Science Foundation of China (U21A20508, 61975208 AND 62105334), the Scientific Instrument Development Project of the Chinese Academy of Science (YZLY202001), Fujian Science & Technology Innovation Laboratory for Optoelectronic Information of China (2021ZR203, 2020ZZ108, and 2021ZZ118), and the Project of Science and Technology of Fujian Province (2021H0047).

**Data availability** The data that support the findings of this study are available from the corresponding authors upon reasonable request.

## Declarations

**Conflict of interest** The authors declare that they have no known competing financial interests or personal relationships that could have appeared to influence the work reported in this paper.

## References

1. G.D. Boyd, H. Kogelnik, *Bell Syst. Tech. J.* **41**, 1347 (1962)
2. Y.-F. Chen, C.-H. Wang, X.-L. Zheng, M.-X. Hsieh, *Appl. Sci.* **11**, 8913 (2021)
3. S.-C. Chu, Y.-T. Chen, K.-F. Tsai, K. Otsuka, *Opt. Express* **20**, 7128 (2012)
4. A. Hu, J. Lei, P. Chen, Y. Wang, S. Li, *Appl. Opt.* **53**, 7845 (2014)
5. F. Schepers, T. Bexter, T. Hellwig, C. Fallnich, *Appl. Phys. B* **125**, 75 (2019)
6. M. Dienerowitz, M. Mazilu, P.J. Reece, T.F. Krauss, K. Dholaikia, *Opt. Express* **16**, 4991 (2008)
7. S. Fühapter, A. Jesacher, S. Bernet, M. Ritsch-Marte, *Opt. Lett.* **30**, 1953 (2005)
8. Y.F. Chen, Y.P. Lan, *Appl. Phys. B* **73**, 11 (2001)
9. H.-H. Wu, W.-F. Hsieh, *J. Opt. Soc. Am. B* **18**, 7 (2001)
10. Y.F. Chen, Y.P. Lan, *Phys. Rev. A* **65**, 013802 (2001)
11. C.-H. Chen, P.-T. Tai, W.-F. Hsieh, *Opt. Commun.* **241**, 145 (2004)
12. V.V. Bezotosnyi, E.A. Cheshev, M.V. Gorbunkov, P.V. Kostryukov, V.G. Tunkin, *Appl. Opt.* **47**, 3651 (2008)
13. Y. S. Yijie Shen, Z. W. Zhensong Wan, X. F. Xing Fu, and M. G. Mali Gong, *Chin. Opt. Lett.* **17**, 031404 (2019).
14. M.V. Gorbunkov, P.V. Kostryukov, V.G. Tunkin, *Laser Phys.* **29**, 115003 (2019)
15. Z.-D. Cheng, Z.-D. Liu, X.-W. Luo, Z.-W. Zhou, J. Wang, Q. Li, Y.-T. Wang, J.-S. Tang, J.-S. Xu, C.-F. Li, G.-C. Guo, *Opt. Lett.* **42**, 2042 (2017)
16. Chr. Tamm, *Phys. Rev. A* **38**, 5960 (1988).
17. C. Tradonsky, M. Nixon, E. Ronen, V. Pal, R. Chriki, A.A. Friesem, N. Davidson, *Photonics Res.* **3**, 77 (2015)
18. Y.F. Chen, Y.H. Hsieh, J.C. Tung, H.C. Liang, K.F. Huang, E.P.L. Europhys. Lett. **122**, 30002 (2018)
19. J.C. Tung, P.H. Tuan, H.C. Liang, K.F. Huang, Y.F. Chen, *Phys. Rev. A* **94**, 023811 (2016)
20. X.L. Zheng, M.X. Hsieh, Y.F. Chen, *Opt. Lett.* **47**, 2518 (2022)
21. T.H. Lu, Y.C. Lin, Y.F. Chen, K.F. Huang, *Appl. Phys. B* **103**, 991 (2011)
22. Y.F. Chen, C.H. Jiang, Y.P. Lan, K.F. Huang, *Phys. Rev. A* **69**, 053807 (2004)
23. V.V. Bezotosnyi, E.A. Cheshev, M.V. Gorbunkov, A.L. Koromyslov, P.V. Kostryukov, M.S. Krivonos, Y.M. Popov, V.G. Tunkin, *Laser Phys. Lett.* **12**, 025001 (2015)
24. Y.F. Chen, T.H. Lu, K.W. Su, K.F. Huang, *Phys. Rev. Lett.* **96**, 213902 (2006)
25. Y.F. Chen, C.C. Lee, C.H. Wang, M.X. Hsieh, *Chin. Opt. Lett.* **18**, 091404 (2020)
26. J. Dingjan, M.P. Van Exter, J.P. Woerdman, *Opt. Commun.* **188**, 345 (2001)
27. A.E. Siegman, *Lasers* (University Science Books, Mill Valley, California, 1986)
28. Y.F. Chen, S.C. Li, Y.H. Hsieh, J.C. Tung, H.C. Liang, K.F. Huang, *Opt. Lett.* **44**, 2649 (2019)
29. Y.F. Chen, T.M. Huang, K.H. Lin, C.F. Kao, C.L. Wang, S.C. Wang, *Opt. Commun.* **136**, 399 (1997)

30. H. Laabs, B. Ozygus, Opt. Laser Technol. **28**, 213 (1996)

author(s) or other rightsholder(s); author self-archiving of the accepted manuscript version of this article is solely governed by the terms of such publishing agreement and applicable law.

**Publisher's Note** Springer Nature remains neutral with regard to jurisdictional claims in published maps and institutional affiliations.

Springer Nature or its licensor (e.g. a society or other partner) holds exclusive rights to this article under a publishing agreement with the